♥ Cite This: Mol. Pharmaceutics 2019, 16, 3178–3187

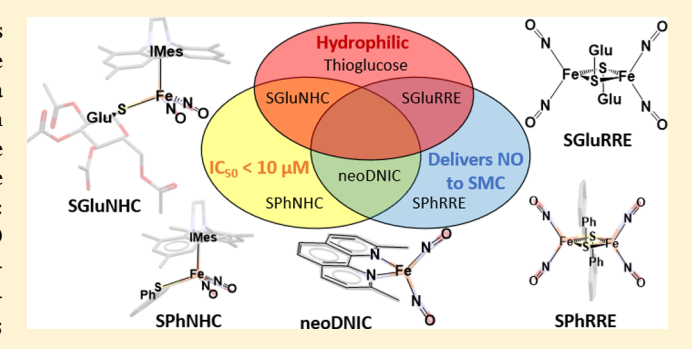
Toward the Optimization of Dinitrosyl Iron Complexes as Therapeutics for Smooth Muscle Cells

D. Chase Pectol, ** Sarosh Khan, **, Rachel B. Chupik, Mahmoud Elsabahy, **, Karen L. Wooley, **, Sarosh Khan, Alandaria Y. Darensbourg, **, and Soon-Mi Lim**, Mahmoud Elsabahy, Karen L. Wooley, **, Sarosh Khan, Alandaria Y. Darensbourg, **

†Departments of Chemistry, [‡]Chemical Engineering, [§]Materials Science & Engineering, and ^{||}The Laboratory for Synthetic-Biologic Interactions, Texas A&M University, College Station, Texas 77842-3012, United States

Supporting Information

ABSTRACT: In this study, dinitrosyl iron complexes (DNICs) are shown to deliver nitric oxide (NO) into the cytosol of vascular smooth muscle cells (SMCs), which play a major role in vascular relaxation and contraction. Malfunction of SMCs can lead to hypertension, asthma, and erectile dysfunction, among other disorders. For comparison of the five DNIC derivatives, the following protocols were examined: (a) the Griess assay to detect nitrite (derived from NO conversion) in the absence and presence of SMCs; (b) the 3-(4,5-dimethylthiazol-2-yl)-5-(3-carboxymethoxyphenyl)-2-(4sulfophenyl)-2H-tetrazolium (MTS) assay for cell viability; (c) an immunotoxicity assay to establish if DNICs stimulate



immune response; and (d) a fluorometric assay to detect intracellular NO from treatment with DNICs. Dimeric Roussin's red ester (RRE)-type $\{Fe(NO)_2\}^9$ complexes containing phenylthiolate bridges, $[(\mu-SPh)Fe(NO)_2]_2$ or **SPhRRE**, were found to deliver NO with the lowest effect on cell toxicity (i.e., highest IC₅₀). In contrast, the RRE-DNIC with the biocompatible thioglucose moiety, $[(\mu\text{-SGlu})\text{Fe}(\text{NO})_2]_2$ (SGlu = 1-thio- β -D-glucose tetraacetate) or SGluRRE, delivered a higher concentration of NO to the cytosol of SMCs with a 10-fold decrease in IC_{50} . Additionally, monomeric DNICs stabilized by a bulky N-heterocyclic carbene (NHC), namely, 1,3-bis(2,4,6-trimethylphenyl)imidazolidene (IMes), were synthesized and yielded the DNIC complexes SGluNHC, [IMes(SGlu)Fe(NO)₂], and SPhNHC, [IMes(SPh)Fe(NO)₂]. These oxidized ${\rm Fe(NO)_2}$ NHC DNICs have an IC₅₀ of ~7 $\mu{\rm M}$; however, the NHC-based complexes did not transfer NO into the SMC. Per contra, the reduced, mononuclear {Fe(NO)₂}¹⁰ neocuproine-based DNIC, neoDNIC, depressed the viability of the SMCs, as well as generated an increase of intracellular NO. Regardless of the coordination environment or oxidation state, all DNICs showed a dinitrosyl iron unit (DNIU)-dependent increase in viability. This study demonstrates a structure-function relationship between the DNIU coordination environment and the efficacy of the DNIC treatments.

KEYWORDS: DNIC, dinitrosyl iron complex, nitric oxide, NORM, nitric oxide release molecule, smooth muscle cells, RAW 264.7, immunotoxicity, cytokine response, metallodrugs

1. INTRODUCTION

Downloaded via TEXAS A&M UNIV COLG STATION on July 24, 2019 at 20:52:18 (UTC). See https://pubs.acs.org/sharingguidelines for options on how to legitimately share published articles.

Nitric oxide (NO) has achieved celebrity status in the last decades for its myriad functions, such as gaseous signaling in mammalian, plant, and bacterial cells that control such things as blood vessel dilation, muscle relaxation, nervous system function, immune response, memory, cell signaling, and posttranslational modification of proteins. 1,2 NO is clearly of importance to physiological/biological chemistry. NO is also a well-studied ligand in coordination chemistry because of its multiple accessible redox levels, a feature related to its ability to delocalize metal d-electrons and participate in $d_{\pi} - \pi^*$ bonding. To account for this delocalization, a notation was created that enumerates the total number, n, of electrons within the $d_{\pi}-\pi^*$ manifold: $\{M(NO)_x\}^n$, where x is the number of nitrosyl ligands.³ The functions of NO in an organism are largely dependent on its concentration. In the picomolar to nanomolar range, NO has therapeutic effects, such as smooth muscle

relaxation, wound healing, nervous system signaling, and proliferation of certain cell types. However, at micromolar levels, NO can trigger apoptosis, damage DNA, indiscriminately nitrosylate protein thiols, and generate reactive oxygen species (ROS) and reactive nitrogen species (RNS).4

The main cellular targets for NO are cysteine, thiols, tyrosine, oxygen, Fe-S clusters, and metal hemes.⁵ Endogenously generated NO arises from three enzymes: endothelial NO synthase (eNOS) is the primary source of NO for smooth muscle cells (SMCs); inducible NOS is involved in immune response; and neuronal NOS is used for nervous system signaling. All forms of NOS generate NO from

Received: April 8, 2019 Revised: May 30, 2019 Accepted: June 5, 2019 Published: June 5, 2019

L-arginine and oxygen in an NAD(P)H-dependent process.^{8,9} Hence, efforts to study the effect of exogeneous NO are to be approached with caution as concomitant changes in endogenous production in response to the treatment can render interpretation of the results ambiguous.

NO is a ubiquitous signaling molecule, with the main target of NO produced from eNOS being soluble guanylate cyclase (sGC). SGC is an Fe-heme containing protein that catalyzes the formation of 3',5'-cyclic guanosine monophosphate from guanosine triphosphate, which is initiated by NO in SMCs. The resultant cascade of events ultimately causes smooth muscle relaxation. NO is not directly delivered to the SMCs but diffuses from the endothelial cells to the SMCs in response to shear stress. Therefore, finding new therapeutics that can deliver a controlled amount of NO would be useful for treating ailments, such as hypertension, asthma, erectile dysfunction, diabetes, or other disorders linked to the improper function of vasculature. 10

NO release molecules (NORMs) are one method of treating these disorders. Organic-based small-molecule NORMs, including NONOates and S-nitrosothiols, are challenged by short half-lives $(t_{1/2})$ of NO release (on the order of minutes for S-nitroso-N-acetyl-DL-penicillamine, DEANO, and similar derivatives) and temperature/light sensitivity (S-nitrosoglutathioine must be stored in the dark at $-80\,^{\circ}$ C). The incorporation of NONOates into larger macrocycles has been shown to abrogate such shortcomings of organic NORM's. Metal-based NORMs exist and have been used as emergency treatments for rapid induction of hypotension, but the most widely used complex, sodium nitroprusside (Na₂[Fe(NO)(CN)₅]), has hazardous side effects, namely, cyanide poisoning. A

The interplay between iron and NO in biology is extensive, including the FeNO-heme and the lesser known dinitrosyl iron complexes (DNICs). The DNICs were first observed in 1964-65 in tissues isolated from rats that had been under oxidative stress. A characteristic electron paramagnetic resonance (EPR) signal at g-value 2.03 would later be identified as a monomeric $\{Fe(NO)_2\}^9$ DNIC with the formula $[(RS)_2Fe(NO)_2]^-$, where SR^- = cysteine/glutathione. ^{15–17} The chemical composition of an EPR-silent type of DNIC is a dimer of {Fe(NO)₂}⁹ dinitrosyl iron units (DNIUs) with bridging thiolates (Roussin's red erster—RRE), 18 which are spin coupled to achieve diamagnetism. Another well-known derivative is Roussin's black salt—RBS¹⁹ existing in the form of Fe₄S₃ clusters that contain three DNIUs and one mononitrosyl iron unit all bridged by sulfides. The connection between such chemical and biological dinitrosyl compositions has been bridged by Foster and Cowan and Ding et al. who demonstrated that NO reacts with Fe_xS_x clusters to produce protein-bound DNICs that are transformed back into Fe,S, clusters with the aid of cysteine desulfurase, which has been corroborated by chemical experiments.²² An extensive and recent review of the history and application of DNICs to biological systems has been assembled by W-F. Liaw and coworkers.²³ As DNICs are expected to be NO storage and transfer agents in biology,²⁴ the question we chose to address is whether synthetic analogues could serve as an exogenous, longlasting source of NO.

In fact, DNICs are postulated to be the "working form" of NO within the cell.^{24–27} Chemically, the DNIC can act as a donor of NO⁺, NO, and NO⁻²⁸ and S-nitrosate protein thiols in anaerobic and aerobic environments.^{29–31} The enhanced

stability that the iron imparts to the reactive nitrosyl, and its versatility as a NO donor, might allow for phenotypes that were not available for organic-based NO donors, or FDA-approved drugs such as Adempas³² that emulate the release of NO by increasing sGC activity.

Related to our specific choice of ligands in the DNICs of Figure 1 is a report that water-soluble $\{Fe(NO)_2\}^9$ DNICs and

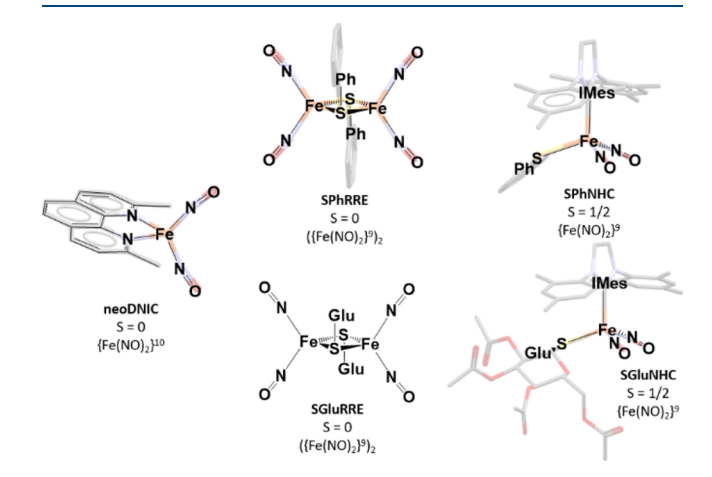


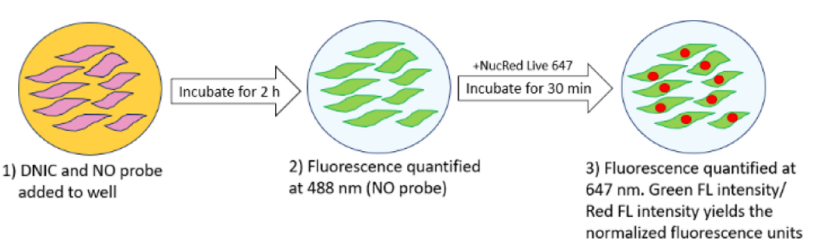
Figure 1. Chemical representations of the DNICs used in this and previous studies.⁴³ SGlu = 1-thio- β -D-glucose tetraacetate; SPh = thiophenol; IMes = 1,3-bis(2,4,6-trimethylphenyl)imidazolidene. *S* is the total electronic spin on the complex. The two $S = 1/2 \{\text{Fe(NO)}_2\}^9$ DNIUs in the RRE DNICs are antiferromagnetically coupled.

RRE-type complexes interact with endothelial cells, HSP70,³³ decrease tumor size in an in vivo rat study,³⁴ and extend the life span of *Caenorhabditis elegans*.³⁵ Extensive in vivo work has shown that glutathionyl DNICs reduce pain in rats,^{36,37} as well as influence platelet aggregation and red blood cell levels.³⁸ Efforts have also been made to synthesize a photoactivated NORM using a DNIC.³⁹ It has also been reported that DNICs can chemically interact with biological analogues of cysteine, Rieske-type iron—sulfur clusters, and tyrosine.^{40,41} In fact, the only X-ray structure of a protein-containing DNIC was obtained from a loading of synthetic glutathione-based RRE-DNIC into glutathione transferase.⁴²

In earlier work, we demonstrated that DNICs containing sugar-appended thiolates increased total nitrite concentration of the cellular media in the presence and absence of endothelial cells and that SGluRRE provided a sustained source of released nitrite into media over 24 h. The N-heterocyclic carbene (NHC)-based complexes and neoDNIC decomposed quickly in an aerobic, aqueous environment. Despite the significance of the effect of NO on SMCs vide supra, DNIC prodrug investigations have relied on endothelial cells.

The array of five DNICs used in this in vitro SMC study is shown in Figure 1. With them, we explore whether NO will be released from its carrier molecule and delivered into the cytosol of SMCs. We probe the coordination environment and oxidation state by contrasting the NHC-based complexes, monomeric $\{\text{Fe}(\text{NO})_2\}^9$ species, with the reduced $\{\text{Fe}(\text{NO})_2\}^{10}$ **neoDNIC**. The enhanced stability of the dimeric complexes, based on μ -SPh and μ -SGlu, offers opportunity to contrast the effect of dinuclearity on NO release; however, dimer splitting by in situ cellular compounds may alter such expectations. Finally, comparison of the effect of RS

Scheme 1. Method of Quantification Used in Detection and Normalization of Intracellular NO



hydrophilicity is possible for both NHC- and RRE-based DNICs. The goal of this research is to study the biological effects of DNICs on smooth muscle and RAW 264.7 cells and to gain a fundamental understanding of the chemical properties of these DNICs that will ultimately lead to effective delivery of NO to the therapeutic target of NO release.

2. EXPERIMENTAL SECTION

2.1. Materials and Characterizations. Chemical syntheses were performed under an N2 atmosphere using standard Schlenk techniques. Solvents used were purified using a Bruker solvent system. The DNICs used in this study (neoDNIC, SPhNHC/RRE, SGluNHC/RRE) were synthesized following published procedures.⁴³ The purities of the complexes were confirmed by solution Fourier transform infrared (FT-IR) spectroscopy (Bruker 37 Tensor FT-IR spectrometer, CaF₂ window, path length = 0.2 mm) and $E\hat{SI}^{+/-}$ -MS (Thermo Scientific Q Exactive Focus. Flow rate = $10 \mu L/min$. Spray voltage = 3.75 kV, and the sheath gas and auxiliary gas flow rates were set to 7 and 0 arbitrary units, respectively. The transfer capillary temperature was held at 250 °C, and the S-Lens RF level was set at 50 V. Exactive Series 2.8 SP1/Xcalibur 4.0 software was used for data acquisition and processing). The 96-well plate colorimetric and fluorometric measurements were performed on a Molecular Devices SpectraMax M5. Clear, sterile, flat-bottomed, 96-well tissue culture plates were used for all bicinchoninic acid, Griess, and 3-(4,5-dimethylthiazol-2-yl)-5-(3-carboxymethoxyphenyl)-2-(4-sulfophenyl)-2H-tetrazolium (MTS) assays. All synthesized or purchased complexes that were used as cell treatments were filtered through sterile 0.2 μ m polyvinylidene fluoride filters before application to cells.

2.2. Cell Culture. Vascular SMCs were kindly gifted by Dr. Andrea Trache at Texas A&M Health Science Center. Cells were isolated from rat cremaster arterioles and were cultured in 5% CO₂ at 37 °C in Dulbecco's modified Eagle medium (DMEM/F12) supplemented with 10% fetal bovine serum (FBS), 10 mM HEPES (Sigma, St. Louis, MO), 2 mM L-glutamine, 1 mM sodium pyruvate, 100 U/mL of penicillin, 100 mg/mL of streptomycin, and 0.25 mg/mL of amphotericin B. Unless otherwise specified, all reagents were purchased from Thermo Fisher Scientific (Waltham, MA).

2.3. Griess Assay. The Griess Reagent Kit was purchased from Biotium and used as directed. The SMCs were plated to confluence in half of the 96 wells on the plate. The medium was aspirated and replaced with the following reagents in each well: $20~\mu\text{L}$ of Griess reagent, $150~\mu\text{L}$ of 1% dimethyl sulfoxide in phenol-free DMEM/F12 solution containing varying concentrations of DNIC, and $130~\mu\text{L}$ of DMEM/F12 (total $300~\mu\text{L/well}$). Absorbance readings at 548 nm of each well after 2, 24, and 48 h of incubation were obtained. The absorbance readings from the wells without cells or Griess

reagent were used as the blanks and subtracted from all absorbance readings.

2.4. MTS Assay. CellTiter 96 AQ One Solution Cell Proliferation Assay was purchased from Promega and used without modification, as described previously. SMCs were grown to confluency, and then they were incubated at 37 °C with DNIC for 72 h. A 20 μ L aliquot of MTS reagent was added to each well and incubated for 2 h. Absorbance was recorded at 490 nm.

2.5. Intracellular NO Detection Using Endpoint Fluorescence. The OxiSelect intracellular NO assay kit (Fluorometric) was purchased from Cell Biolabs and used according to the instructions provided in the kit. The plates used were 96-well Greiner Bio-One Black, F-bottom, FLUOTRAC, high binding, sterile plates. SMCs were plated at 100k/mL and grown overnight in 10% FBS. The following day the medium was aspirated, and the SMCs were incubated with 1-1.5 μ L of DNIC and 1× NO fluorometric probe in phenol-free DMEM/F12 for 2 h in the dark at 37 °C. Fluorometric measurements for the NO probe were obtained (Ex-480 nm/Em-530 nm). Afterward, NucRed live nuclear stain was added to each well as per the instructions provided in the kit and allowed to incubate for 30 min. The fluorometric measurements were then obtained (Ex-638 nm/Em-686 nm). The experimental setup is visualized in Scheme 1. For the DNIC preincubation experiments, DNIC was added 2, 24, and 48 h before incubation with the NO probe for 2 h. DNIC was applied after 2 h NO probe incubation for the NO release profile experiments. Cell fluorescence was also imaged with a laser scanning confocal microscope (Olympus FV 1000) with 10× objective. Cells were plated on eight-well μ -Slides (ibidi, Germany) and treated as described above.

2.6. Multiplex Immunotoxicity Assay. The endotoxin contents of the various DNIC samples were measured by using the Pierce Limulus Amebocyte Lysate Chromogenic Endotoxin Quantitation Kit (Thermo Fisher Scientific Inc., Rockford, IL) according to the manufacturer's instructions, as described previously. 44 RAW 264.7 cells were treated with medium (control), DEANO, neoDNIC, SGluNHC, SGluRRE, SPhNHC, and SPhRRE at 5 μ M for 24 h. RAW 264.7 cells were treated with medium (control), SGluNHC, SGluRRE, and 1-thio- β -D-glucose tetraacetate (thioglucose) at 10 μ M for 24 h. The supernatants were then collected and centrifuged for 10 min at 13 000 rpm. Serial dilutions of standards of cytokines were also prepared in the same diluent utilized for the samples (i.e., cell culture medium). Control, standards, and treated samples (50 μ L) were incubated with antibody-conjugated magnetic beads for 30 min in the dark. After washing the beads, the detection antibody was added to the wells and incubated in the dark for another 30 min under continuous shaking (300 rpm). After washing the beads again, streptavidin-phycoerythrin was added to every well and

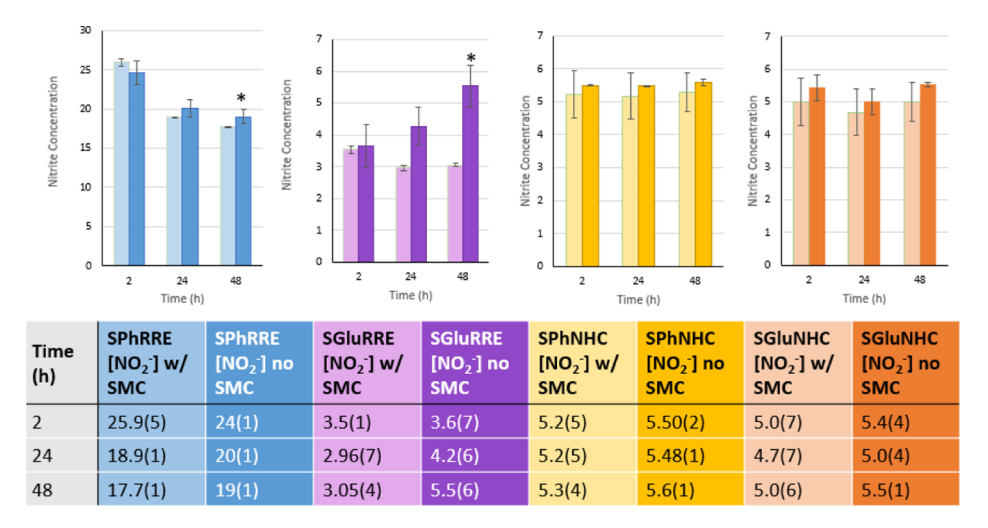


Figure 2. Griess assay results for four DNICs used in this study. The *y*-axis is the concentration of nitrite (μ M) detected in the media. The DNIC concentrations for each trial are 30 μ M. In this figure and throughout the article, **SPhRRE** = blue, **SGluRRE** = purple, **SPhNHC** = yellow, **SGluNHC** = orange. The absorbance was recorded at three separate time points (2, 24, and 48 h) for two separate treatment conditions (without SMCs—dark, with SMCs—light). The same plate was used for the duration of the study. Numbers in parenthesis indicated standard deviation from n = 3 trials. Asterisk indicates p < 0.05 when comparing the concentration of nitrite detected in the presence and absence of cells at that time point and concentration.

incubated while protected from light for 10 min under the same shaking conditions. Finally, after several washings with resuspension in the assay buffer and shaking, the expression of the mouse cytokines, interleukin (IL)- 1α , IL- 1β , eotaxin, granulocyte-colony-stimulating factor (G-CSF), granulocyte macrophage-colony-stimulating factor (GM-CSF), interferon- 1β , keratinocyte-derived chemokine (KC), monocyte chemotactic protein (MCP)- 1β , regulated upon activation normal T-cell expressed and presumably secreted (RANTES), and tumor necrosis factor- 1β , was measured immediately using the Bio-Plex 200 system with HTF and Pro II Wash Station, and the data were analyzed using the Bio-Plex Data Pro software (Bio-Rad Laboratories, Hercules, CA).

Values in Figure 5 are presented as mean \pm SD of three replicates. Significant differences between two groups were evaluated by Student's *t*-test (unpaired) or between more than two groups by one-way analysis of variance, followed by Tukey's multiple comparison tests. Differences between different groups were considered significant for *p* values less than 0.05.

3. RESULTS AND DISCUSSION

3.1. Total Nitrite Detected Using the Griess Assay in the Presence and Absence of SMCs. In vitro detection of formation of nitrite in the cellular media was achieved using the Griess assay, a colorimetric detection of an azo-dye that is only formed in the presence of nitrite. It is established that NO in the presence of oxygen and water converts into NO₂^{-,45} but it is also possible that a NO⁺ ion is hydrolyzed from the DNIC to form nitrite.²⁵ An assay was designed to compare the amount of dye formed in the presence and absence of SMCs. Figure 2 displays the concentration of nitrite detected in the media following incubation of the DNIC at different time periods (2, 24, and 48 h). The amount of nitrite detected from the monomeric NHC DNICs remained constant throughout the time course of the experiment, and there was no difference in the nitrite detected in the presence and absence of SMCs,

which is consistent with our findings in the endothelial cell study.⁴³

In contrast, the RRE DNICs showed a significant increase (p < 0.05) in the amount of nitrite detected in the absence of cells after 24 h (SPhRRE) or 48 h (SGluRRE). Besides the statistically higher amount of nitrite detected without cells, each dimer showed a different release profile to the SMCs. SGluRRE exhibited a steady increase in the concentration of nitrite detected in the absence of cells, but in the presence of cells, the amount of nitrite detected remained constant. The other dimeric complex SPhRRE did not show the same increase in nitrite concentration over time, but in the absence of SMCs, [NO₂⁻] was higher than in the presence of SMCs. This study provides information about the amount of nitrite present in the extracellular environment upon treatment with DNICs but provides no information regarding NO transfer into the cells. From these data, we can conclude that the DNICs result in nitrite detection in the extracellular environment and that the presence of SMCs causes a decrease in the amount of nitrite detected for the RRE DNICs.

3.2. Effect of the DNIC Treatments on Cell Viability. In the next set of experiments, we investigated which features of the DNICs had the greatest effect on the viability of SMC's. The viability was determined colorimetrically by observing the presence of a formazan dye, which is reduced from a tetrazole in the MTS assay by mitochondrial reductases. Unexpectedly, the DNICs and/or their byproducts resulted in significant increases in viabilities at relatively low concentrations. Therefore, the experiments were conducted in triplicate for three separate runs for each DNIC. The viability curves shown in Figure 3 are representative of three independent trials, the only exception being SPhRRE (see Figure S1). To account for the apparent systematic increases in viabilities, the IC₅₀ values were calculated from fitting logarithmic trendlines through the linear effect ranges with the IC₅₀ concentrations being calculated at half of the maximum observed viabilities.

The monomeric DNICs (**neoDNIC**, **SGluNHC**, **SPhNHC**) have similar IC_{50} s regardless of coordination environment, thiol functionality, or oxidation state of the DNIC source. The

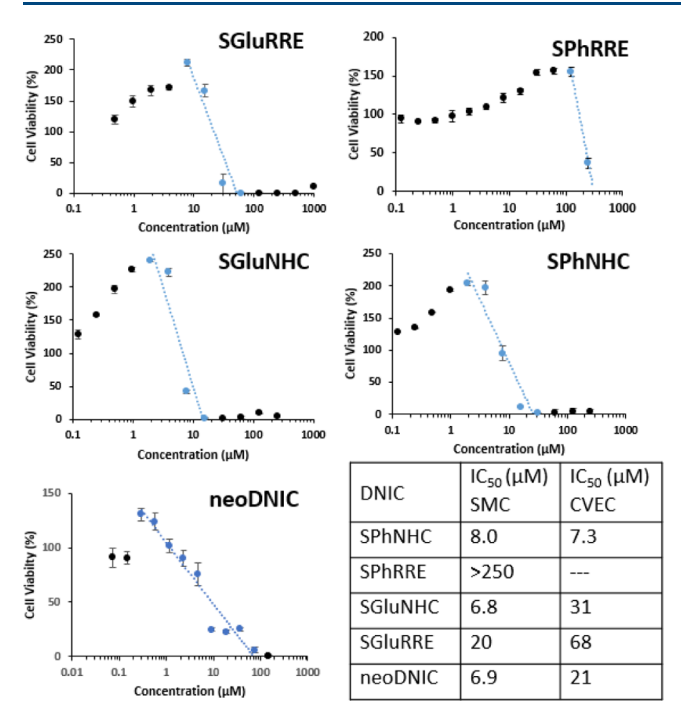


Figure 3. Results of viability assay for SMCs treated with DNICs. Trials shown are representative of three independent trials. The IC_{50} values in the table are calculated based on the plots shown in this figure. The trendlines were used to calculate the IC_{50} . Values from previous study with CVECs are compared.⁴³

higher IC_{50} values of the dimeric DNICs as compared to the monomeric DNICs are attributed to the stability of the dimeric DNIU in solution compared to the monomeric counterparts. The single outstanding difference was thiol functionality on the RREs. By changing the thiol identity from thiophenol to thioglucose, the IC_{50} decreased approximately 10-fold from >250 μ M (SPhRRE) to 20 μ M (SGluRRE).

It is notable that the IC_{50} values from the coronary venular endothelial cell (CVEC) study⁴³ are generally higher compared to that of the SMC study, with the sole exception being **SPhNHC**. A supposition is that as the endothelial cells generate NO from eNOS, they are more resistant to RNS when compared to SMCs, which are the ultimate therapeutic target of the endothelial cell-generated NO.

It was established that the observed increase and decrease in viability was due to the DNIC and not its major decomposition products (Figure 4). The carbene and the thiols relevant to the DNIC and **DEANO**, the positive control for NO release, are overlaid with the DNIC viability curves. These decomposition products do not result in an increase in viability of the cells; instead, they become toxic to the SMC at higher concentrations (\sim 500 μ M). In contrast, all of the DNIC treatments exhibit an increase in viability, followed by a stark, concomitant decrease. While the mechanism by which these DNICs increase cell viability is undetermined, we can say that in SMCs the DNIU is responsible for the observed increase in mitochondrial reductase activity.

3.3. Investigations of the Effect of DNICs on Immune System Activity. The use of DNICs as drugs requires an understanding of how they affect the viability of individual cells and, in addition, how the DNICs might stimulate the immune system toward action. Cytokines are known to be involved with communication between different actors in the immune system. Measurement of the expression of various cytokines⁴⁶

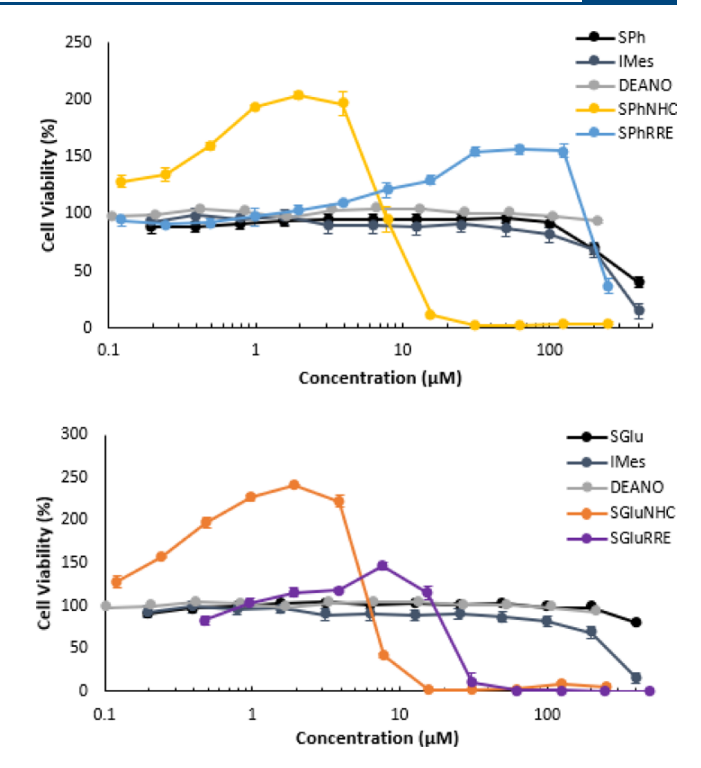


Figure 4. Overlaid results of the viability assay for SMC treated with DNICs and their decomposition products. The thioglucose containing DNICs are in the top panel, and the thiophenol DNICs are on the bottom. IMes, SGlu, and SPh are the ligands used to synthesize the DNICs as shown in Figure 1.

is usually utilized to demonstrate the ability of biomaterials to interact with the immune system either in vitro or in vivo. 44,47-50 For example, a number of the IL cytokines could be responsible for recruiting macrophages, starting an inflammatory response, or activating T-cells toward action. 51 Recently, an immunotoxicity index was developed to facilitate interpretation of the expression of cytokines from biological systems. 52 After measurement of cytokines for different treatments, overexpression of cytokines was compared to the control untreated group (p < 0.05). Values exceeding 1 (i.e., higher than the control) are summed and used as numerical theoretical values for evaluating the immunotoxicity of the tested materials (i.e., the higher the index value, the higher the predicted immunotoxicity). It is worth mentioning that the concentration of DNIC at which the immunotoxicity index is calculated must be provided because the index value depends on the concentration of the tested materials. The concentration used for these immunotoxicity assays was determined using the IC50 values for the array of DNIC complexes on RAW 264.7 cells (Figure S2). Also, the duration of the treatment must be fixed. In this particular study, there was no need to evaluate the potential adsorption of the measured cytokines onto the tested materials because the materials tested here are small molecules rather than particles, which are unlikely to result in significant adsorption of the measured cytokines. 53,54

From the viability curves (Figure S2), it was determined that the monomeric DNICs (neoDNIC, SGlu/SPhNHC) were highly toxic to macrophages, with IC₅₀s in the high nanomolar range (Table 1). On the other hand, the dimeric DNICs SGlu/SPhRRE were less toxic, with IC₅₀s in the high micromolar range. In contrast to the behavior of SMCs treated with

Table 1. Calculated IC₅₀ Values for RAW 264.7 Cells Treated with DNICs^a

DNIC/NO source	IC ₅₀ (μM) RAW 264.7
SPhNHC	0.29
SPhRRE	>250
SGluNHC	0.12
SGluRRE	210
neoDNIC	0.37
DEANO	110

^a**DEANO** was used as the positive control for NO release.

DNICs, the macrophages did not exhibit an increase in viability upon DNIC treatment.

No detectable amounts of endotoxins were identified in the DNIC samples (data not shown). **DEANO**, **neoDNIC**, **SGluNHC**, **SGluRRE**, **SPhNHC**, and **SPhRRE** had immunotoxicity indices of 2.5, 0, 0, 12.6, 0, and 7.7, respectively, at the concentration of 5 μ M (Figure 5). On the basis of previous

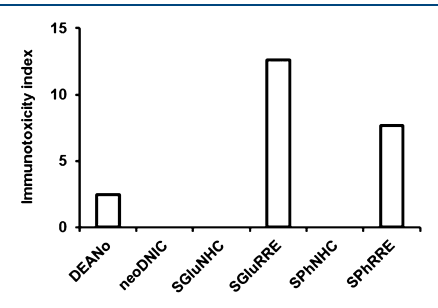


Figure 5. Calculated immunotoxicity index for the induction of mouse cytokines IL-1 α , IL-1 β , IL-2, IL-3, IL-4, IL-5, IL-6, IL-9, IL-10, IL-12 (P40), IL-12 (P70), IL-13, IL-17, eotaxin, G-CSF, GM-CSF, IFN- γ , KC, MCP-1, MIP-1 α , MIP-1 β , RANTES, and TNF- α following the treatment of RAW 264.7 cells with **DEANO**, **neoDNIC**, **SGluNHC**, **SGluRRE**, **SPhNHC**, and **SPhRRE** at 5 μ M for 24 h.

testing of various drugs and polymeric materials, an immunotoxicity index below 15 is considered to have minimal immunotoxicity, from 15 to 45 is considered moderate, and above 45 would be considered severe. Out of the 23 measured cytokines, slight induction was observed only for RANTES (Tcell recruitment) and TNF- α (apoptosis signal) after treatment with SGluRRE and SPhRRE (Figure S3), whereas no cytokines were significantly induced after treatment with neoDNIC, SGluNHC, and SPhNHC. On the basis of previously published data and other tested materials, these complexes at the tested concentrations are considered to have minimal immunotoxicity. 44,47-50 It is worth mentioning that the low IC₅₀ measured in RAW 264.5 macrophages following treatment with neoDNIC, SGluNHC, and SPhNHC might have contributed to the observed decease in the production of the cytokines, as compared to the control untreated cells. On the basis of preliminary experiments, the concentration of 5 µM was the minimal concentration that can be utilized to observe an increase in cytokines release in response to the treatment with the complexes, as compared to the control untreated cells.

3.4. Fluorometric Methodology and Analysis of Intracellular NO. *3.4.1. Confocal Microscopy.* The OxiSelect NO probe was used to examine the hypothesis that the difference in observed nitrite in the presence versus in the absence of SMCs from the Griess assay might be due to some

loss of the NO payload via delivery and ultimately consumption inside the cells. The DNICs that exhibited a statistically significant increase (SGluRRE, SPhRRE) in nitrite detected in the absence of cells would be expected to show an increase in intracellular NO concentration. None of the compounds absorbed or emitted in such a way that would interfere with the fluorescence measurements. In order to better visualize the intracellular NO probe, the SMCs in Figures S4 and S5 were pretreated with the NOS inhibitor L-NNA. The resulting fluorometric images show the holistic differences between SMC populations treated with the NO probe and DNIC for 2 h (Figure S4). The most obvious difference was observed for neoDNIC, where after treatment, there was a visible increase in intensity with the cells being marked by bright green puncta. The monomeric NHC DNICs and SPhRRE did not show a difference that could be detected without the aid of further quantification (Figures S4 and S5). There were some brighter patches of green fluorescence visible in the confocal images of SMCs treated with SGluRRE. In order to properly quantify the amount of fluorescence, the needed normalization factors for the total number of cells were obtained from the fluorometric assay, as described below.

3.4.2. Quantification of Intracellular NO from the Fluorometric Assay. Scheme 1 represents the method adopted for detection and quantification of intracellular NO. Normally for such assays, a cell counting step is incorporated at the end of the experiment; however, as these fluorescence assays take place in an opaque, black-bottomed 96-well plate, the normal colorimetric spectroscopic methods cannot be implemented. Hence, in order to quantify the total cell population in these conditions, a nuclear stain for live cells with an excitation and emission well beyond the range of the green fluorescent probe was used (NucRed647). By dividing the total green fluorescence (amount of intracellular NO detected by the probe) by the red fluorescence (number of nuclei present in each sample well), the average intracellular NO per individual cell was obtained. This approach does not determine whether the DNIC enters the cytosol, but it does provide a definitive conclusion about the released NO. It has been established that DNICs can liberate NO⁺, NO, or NO⁻ depending on the identity of the ligand that exchanges or displaces the NO on iron with NO.²

By using this normalized total fluorescence, the difference between the fluorescence signal generated by SMCs that received no treatment and those that received DNIC treatment could be determined. Three general methods were applied (Figure 6A). Coincubation is described as the simultaneous application of the DNIC and NO probe to the SMCs (Figure 6B,C). For preincubation, the DNIC was applied to the SMCs 2, 24, or 48 h before the NO probe was added (Figure 6D). Last, in the NO release profile experiments, the NO probe was incubated with SMCs for 2 h, and then the DNIC was added to the SMC and fluorescence was measured every 45 s after DNIC treatment (Figure 6E,F). **DEANO** (10 μ M) was used as the positive control for NO release for these experiments. In Figure 6B, the normalized fluorescence (488 nm/647 nm) was observed after 2 h treatment with the five DNICs in this study.

On the basis of the results, neither SGluNHC nor SPhNHC caused a change in the total intracellular NO. While the method by which these complexes elicit a lethal response in the SMC requires further investigation, we can conclude from these data that the NHC-based DNICs did not deliver their NO payload inside the cell. On the basis of the Griess assay

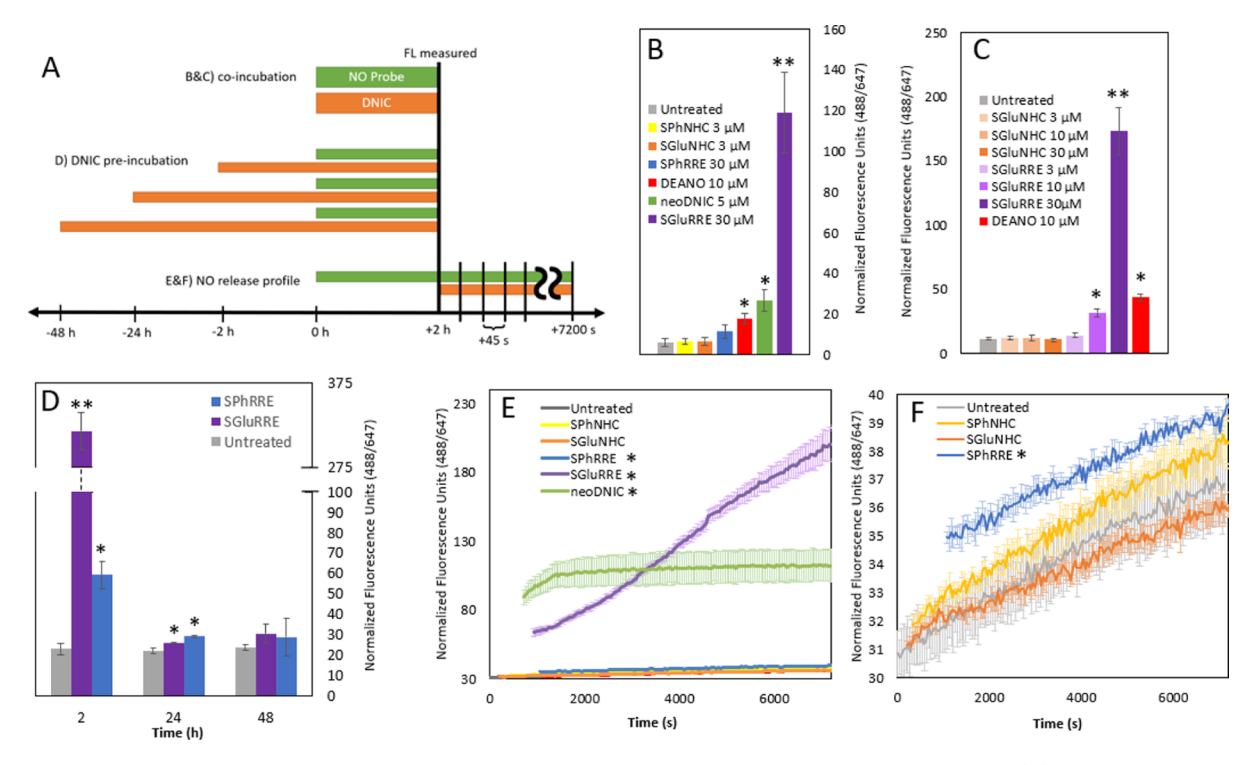


Figure 6. Fluorometric detection and quantification of intracellular NO using the OxiSelect intraNO probe. (A) Diagram of difference in incubation timeline for different DNIC treatments. (B,C) Quantification of intracellular NO via coincubation with 100 μM L-NNA (NOS inhibitor). Cells were incubated with the probe and the DNIC treatment for 2 h at 37 °C. Differences in cell population were normalized with NucRed live stain. (D) Time-dependent fluorescence quantification of DNIC preincubation for 2, 24, or 48 h. (E,F) NO release profile of the five DNICs with the same concentrations used in the previous experiment. Time = 0 indicates the time point at which SMCs were initially treated with DNIC. Asterisk indicates p < 0.05 when comparing the fluorescence values to control. Double asterisk indicates p < 0.01.

Table 2. Summary of the Structure-Function Relationships of the Five DNIC Complexes^a

	SGluRRE	SGluNHC	SPhRRE	SPhNHC	neoDNIC
Redox level of DNIC source	{Fe(NO) ₂ } ⁹	{Fe(NO) ₂ } ⁹	{Fe(NO)₂}9	{Fe(NO)₂}9	{Fe(NO) ₂ } ¹⁰
Nuclearity	Dimer	Monomer	Dimer	Monomer	Monomer
Thiol identity	Glucose	Glucose	Phenyl	Phenyl	N/A
SMC IC ₅₀ (μM)	20	6.8	>250	7-3	6.9
RAW 264.7 IC ₅₀ (μM)	210	0.12	>250	0.29	0.37
NO into cytosol	Yes	No	Yes	No	Yes
Immunotoxicity index	Minimal (12.6)	None (o)	Minimal (7.7)	None (o)	None (o)

^aHighlighted columns represent DNIC-based therapeutics of greatest promise.

(Figure 2) and the data presented in Figure 6B,C, we posit that either the NHC-based DNICs released/degraded too quickly and did not gain entry into the cytosol even at higher concentrations (Figure 6C) or the NHC-based complexes, upon entry into the cell, could have generated a nitroso-iron species that was unable to liberate NO. The liberated NO could have diffused from solution⁵⁵ or decomposed in the extracellular matrix, but it did not enter the cell as NO.

In contrast, the dimeric RRE complexes delivered NO into the cytosol, and the thiosugar-appended **SGluRRE** imported approximately 6× more NO into the cell after 2 h than did the simple thiophenol-appended **SPhRRE** (Figure 6B). **SPhRRE** apparently produced an increase in intracellular NO; however, it was not statistically significant. With **SGluRRE** and **neoDNIC**, there were significant increases in the intracellular

NO concentration. This import or delivery was also concentration-dependent (Figure 6C). If the SMCs were preincubated with DNIC before treatment with the NO probe, a statistically significantly higher intracellular NO concentration remained present 24 h after treatment with DNIC. After 48 h, there was no longer a difference between the intracellular NO concentrations (Figure 6D). SGluRRE produced a higher concentration inside the cell compared to SPhRRE at the 2 h time point, but after 24 h, the intracellular NO concentrations from both complexes were similar. The thiosugar moiety on SGluRRE led to the DNIC treatment releasing more of its NO into the cytosol. It is expected that the sugar group caused the DNIC to be actively transported into the cell, a supposition that is supported by the drastic increase of intracellular NO at 2 h. Observing the NO release

profiles of the five tested DNICs shows definitively that SGlu/SPhNHC does not release NO into the cytosol, and SPhRRE treatment causes a small increase in the intracellular NO (Figure 6F). The neoDNIC-treated cells reached their maximum at 1500 s, further reinforcing that it delivers its NO rapidly. On the other hand, SGluRRE provided a sustained release of NO over the 2 h observation period (Figure 6E).

3.5. Comments and Conclusion. From this study, we conclude that both dimeric complexes, SGluRRE and SPhRRE, are more promising prodrug systems than are the NHC-based monomeric counterparts. Although their ultimate fate is unknown, it is understood that the dimeric complexes provide a source of NO to SMCs that is sustained over 24 h, while exhibiting limited cytotoxicity and generating minimal immunotoxic effects. The thioglucose functionality of SGluRRE gave increased NO delivery to the cytosol versus SPhRRE, with only minor reduction in IC₅₀. Moreover, SGluRRE induced no cytokine response from RAW 264.7 cells, and the monomeric SGluNHC induced a cytokine response minimally. From this, we conclude that there is no artificial stimulation of the immune system for these complexes (Table 2). For mononuclear DNICs, the reduced $\{Fe(NO)_2\}^{10}$ source (neoDNIC) is a more effective vehicle for NO delivery in an in vitro environment when compared to the oxidized DNIC sources (SGlu/SPhNHC). The Griess assay determined that the concentration of NO-derived nitrite in the media decreased in the presence of cells, leading to the conclusion that the SMCs consume the DNICs.

This study offers initial clues into the rational design of small-molecule DNICs appropriate for NO delivery. For this series, the stability provided by the multinuclear nature of the RRE DNICs is the determining factor for sustained release of NO. As the RRE-type complexes are neutral, their in vitro reactivity can be modified by altering the substituents on the thiol. Appending more polar groups to the thiol should aid in its water solubility, which may be of importance in developing therapeutics. Additionally, lipophilic moieties or compounds known to be actively transported across cell membranes might be added to increase the DNICs cell permeability. Such derivatives await future studies.

What is evident from these experiments is that the dimeric DNICs and **neoDNIC** are prodrugs for NO release, and these specific NHC-based DNICs are not. The composition of the complex responsible for ultimately releasing the NO (i.e., intact RRE dimer, some derivatives of the diiron species, or a monomeric DNIC generated in situ) has yet to be identified. We continue to develop hypotheses and experiments to probe the nature of the active species.

Although not all of the DNIC derivatives delivered NO into the cytosol, all increased the viability in SMC that was shown to be an NO-independent process. However, the toxicity of the monomeric NHC-based DNICs to macrophages would be a hindrance for their development as proliferative therapeutic agents. In contrast, SGluRRE was shown to be an order of magnitude less toxic to RAW 264.7 when compared to SMC, so it could be used as a proliferative therapeutic without deleterious effects to the immune system. Furthermore, SGluRRE (and may be other DNICs pending the results of the immunotoxicity assay) are not artificially stimulating a cytokine response. From these data, the dimeric RRE-DNIC scaffold seems to be the optimal vehicle for NO release and DNIU-based therapeutics, and the monomeric, reduced DNIU

could potentially be developed further as a vehicle for rapid delivery of NO.

ASSOCIATED CONTENT

S Supporting Information

The Supporting Information is available free of charge on the ACS Publications website at DOI: 10.1021/acs.molpharmaceut.9b00389.

Complete cell viability data and confocal microscopy images for DNIC-treated SMCs and RAW 264.7 cells (PDF)

AUTHOR INFORMATION

Corresponding Authors

- * E-mail: marcetta@chem.tamu.edu (M.Y.D.).
- * E-mail: soonmi.lim@chem.tamu.edu (S.-M.L.).

ORCID ®

D. Chase Pectol: 0000-0003-4026-4900

Marcetta Y. Darensbourg: 0000-0002-0070-2075

Soon-Mi Lim: 0000-0002-7186-4629

Author Contributions

All authors have given approval to the final version of the manuscript.

Funding

Financial support from the National Science Foundation (CHE-1665258) and the Welch Foundation (A-0924) to the M.Y.D. lab and the Welch Foundation (A-0001) to the K.L.W. laboratory is gratefully acknowledged.

Notes

The authors declare no competing financial interest.

ACKNOWLEDGMENTS

The authors thank Dr. Andreea Trache at Texas A&M Health Science Center for her generosity with the rat arteriolar SMCs used in this study. Biological studies were performed at the Laboratory for Synthetic-Biologic Interactions at Texas A&M University.

ABBREVIATIONS

CVEC, coronary venular endothelial cell; **DEANO**, 1,1-diethyl-2-hydroxy-2-nitroso-hydrazine sodium salt; DNIC, dinitrosyl iron complex; DNIU, dinitrosyl iron unit; IL-X, interleukin-X; IMes, 1,3-bis(2,4,6-trimethylphenyl)-imidazolidene; GSNO, S-nitrosoglutathione; L-NNA, L- N^G -nitroarginine; MTS, 3-(4,5-dimethylthiazol-2-yl)-5-(3-carboxymethoxyphenyl)-2-(4-sulfophenyl)-2H-tetrazolium; NHC, N-heterocyclic carbene; NO, nitric oxide; NORM, nitric oxide release molecule; RNS, reactive nitrogen species; RRE, Roussin's red ester; sGC, soluble guanylate cyclase; SGlu, 1-thio- β -D-glucose tetraacetate; SMC, vascular smooth muscle cell; SNAP, S-nitroso-N-acetyl-DL-penicillamine; SPh, thiophenol

REFERENCES

- (1) Leon, L.; Jeannin, J.-F.; Bettaieb, A. Post-translational Modifications Induced by Nitric Oxide (NO): Implication in Cancer Cells Apoptosis. *Nitric Oxide* **2008**, *19*, 77–83.
- (2) Carpenter, A. W.; Schoenfisch, M. H. Nitric oxide release: Part II. Therapeutic applications. *Chem. Soc. Rev.* **2012**, *41*, 3742–3752.

(3) Enemark, J. H.; Feltham, R. D. Principles of Structure, Bonding, and Reactivity for Metal Nitrosyl Complexes. *Coord. Chem. Rev.* **1974**, 13, 339–406.

- (4) Mocellin, S.; Bronte, V.; Nitti, D. Nitric Oxide, a Double Edged Sword in Cancer Biology: Searching for Therapeutic Opportunities. *Med. Res. Rev.* **2007**, *27*, 317–352.
- (5) Martin, E.; Berka, V.; Bogatenkova, E.; Murad, F.; Tsai, A.-L. Ligand Selectivity of Soluble Guanylyl Cyclase Effect of the Hydrogen-bonding Tyrosine in the Distal Heme Pocket on Binding of Oxygen, Nitric Oxide, and Carbon Monoxide. *J. Biol. Chem.* **2006**, 281, 27836–27845.
- (6) Kumar, S.; Singh, R. K.; Bhardwaj, T. R. Therapeutic Role of Nitric Oxide as Emerging Molecule. *Biomed. Pharmacother.* **2017**, *85*, 182–201.
- (7) Zhao, Y.; Brandish, P. E.; Ballou, D. P.; Marletta, M. A.; Howard; Walsh, C. T. A Molecular Basis for Nitric Oxide Sensing by Soluble Guanylate Cyclase. *Proc. Natl. Acad. Sci. U.S.A.* **1999**, *96*, 14753–14758
- (8) Bogdan, C. Nitric Oxide Synthase in Innate and Adaptive Immunity: an Update. *Trends Immunol.* **2015**, *36*, 161.
- (9) Forstermann, U.; Sessa, W. C. Nitric Oxide Synthases: Regulation and Function. *Eur. Heart J.* **2012**, 33, 829–837.
- (10) Brozovich, F. V.; Nicholson, C. J.; Degen, C. V.; Gao, Y. Z.; Aggarwal, M.; Morgan, K. G. Mechanisms of Vascular Smooth Muscle Contraction and the Basis for Pharmacologic Treatment of Smooth Muscle Disorders. *Pharmacol. Rev.* **2016**, *68*, 476–532.
- (11) Mathews, W. R.; Kerr, S. W. Biological activity of S-nitrosothiols: the role of nitric oxide. *J. Pharmacol. Exp. Ther.* **1993**, 267, 1529–1537.
- (12) Huerta, S.; Chilka, S.; Bonavida, B. Nitric Oxide Donors: Novel Cancer Therapeutics. *Int. J. Oncol.* **2008**, *33*, 909–927.
- (13) Jin, H.; Yang, L.; Ahonen, M. J. R.; Schoenfisch, M. H. Nitric Oxide-Releasing Cyclodextrins. J. Am. Chem. Soc. 2018, 140, 14178.
- (14) Tinker, J. H.; Michenfelder, J. D. Sodium Nitroprusside. *Anesthesiology* **1976**, *45*, 340–352.
- (15) Mallard, J. R.; Kent, M. Differences observed between Electron Spin Resonance Signals from Surviving Tumour Tissues and from their Corresponding Normal Tissues. *Nature* **1964**, 204, 1192.
- (16) Lloveras, J.; Vincensini, P.; Ribbes, G.; Record, M.; Ferre, G.; Douste-Blazy, L.; Pescia, J. Subcellular Localization and Paramagnetic Properties of Signals Observed in Krebs II Ascites Cells by Electron Spin Resonance Spectroscopy. *Radiat. Res.* **1980**, 82, 45–54.
- (17) Vithayathil, A. J.; Ternberg, J. L.; Commoner, B. Changes in Electron Spin Resonance Signals of Rat Liver During Chemical Carcinogenesis. *Nature* **1965**, 207, 1246–1249.
- (18) Lu, C.-Y.; Liaw, W.-F. Formation Pathway of Roussin's Red Ester (RRE) via the Reaction of a {Fe(NO)₂}¹⁰ Nitrosyliron Complex (DNIC) and Thiol: Facile Synthetic Route for Synthesizing Cysteine-containing DNIC. *Inorg. Chem.* **2013**, *52*, 13918–13926.
- (19) Hamilton-Brehm, S. D.; Schut, G. J.; Adams, M. W. W. Antimicrobial Activity of the Iron-sulfur Nitroso Compound Roussin's Black Salt [Fe₄S₃(NO)₇] on the Hyperthermophilic Archaeon Pyrococcus Furiosus. *Appl. Environ. Microbiol.* **2009**, 75, 1820–1825.
- (20) Foster, M. W.; Cowan, J. A. Chemistry of Nitric Oxide with Protein-bound Iron Sulfur Centers. Insights on Physiological Reactivity. *J. Am. Chem. Soc.* **1999**, *121*, 4093–4100.
- (21) Rogers, P. A.; Eide, L.; Klungland, A.; Ding, H. Reversible Inactivation of E. coli Endonuclease III via Modification of its [4Fe-4S] Cluster by Nitric Oxide. *DNA Repair* **2003**, *2*, 809–817.
- (22) Schiewer, C. E.; Muller, C. S.; Dechert, S.; Bergner, M.; Wolny, J. A.; Schunemann, V.; Meyer, F. Effect of Oxidation and Protonation States on [2Fe-2S] Cluster Nitrosylation Giving {Fe(NO)2}⁹ Dinitrosyl Iron Complexes (DNICs). *Inorg. Chem.* **2019**, *58*, 769.
- (23) Lu, T.-T.; Wang, Y.-M.; Hung, C.-H.; Chiou, S.-J.; Liaw, W.-F. Bioinorganic Chemistry of the Natural [Fe(NO)₂] Motif: Evolution of a Functional Model for NO-related Biomedical Application and Revolutionary Development of a Translational Model. *Inorg. Chem.* **2018**, *57*, 12425–12443.

- (24) Hickok, J. R.; Sahni, S.; Shen, H.; Arvind, A.; Antoniou, C.; Fung, L. W. M.; Thomas, D. D. Dinitrosyliron Complexes are the Most Abundant Nitric Oxide-Derived Cellular Adduct: Biological Parameters of Assembly and Disappearance. *Free Radical Biol. Med.* **2011**, *51*, 1558–1566.
- (25) Vanin, A. F. Dinitrosyl Iron Complexes with Thiol-containing Ligands as a "Working Form" of Endogenous Nitric Oxide. *Nitric Oxide* **2016**, 54, 15–29.
- (26) Vanin, A. F. Dinitrosyl Iron Complexes with Thiol-containing Ligands as a Base for New-generation Drugs. *Open Conf. Proc. J.* **2013**, 4, 47–53.
- (27) Drapier, J. C.; Pellat, C.; Henry, Y. Generation of EPR-detectable nitrosyl-iron complexes in tumor target cells cocultured with activated macrophages. *J Biol Chem* **1991**, *266*, 10162–10167.
- (28) Lu, T.-T.; Chen, C.-H.; Liaw, W.-F. Formation of the Distinct Redox-interrelated Forms of Nitric Oxide from Reaction of Dinitrosyl Iron Complexes (DNICs) and Substitution Ligands. *Chem.—Eur. J.* **2010**, *16*, 8088–8095.
- (29) Keszler, A.; Diers, A. R.; Ding, Z.; Hogg, N. Thiolate-based dinitrosyl iron complexes: Decomposition and detection and differentiation from S-nitrosothiols. *Nitric Oxide* **2017**, *65*, 1–9.
- (30) Bosworth, C. A.; Toledo, J. C., Jr.; Zmijewski, J. W.; Li, Q.; Lancaster, J. R., Jr. Dinitrosyliron Complexes and the Mechanism(s) of Cellular Protein Nitrosothiol Formation from Nitric Oxide. *Proc. Natl. Acad. Sci. U.S.A.* **2009**, *106*, 4671–4676.
- (31) Li, Q.; Li, C.; Mahtani, H. K.; Du, J.; Patel, A. R.; Lancaster, J. R., Jr Nitrosothiol Formation and Protection Against Fenton Chemistry by Nitric Oxide-induced Dinitrosyliron Complex Formation from Anoxia-initiated Cellular Chelatable Iron Increase. *J. Biol. Chem.* **2014**, 289, 19917–19927.
- (32) Frey, R.; Becker, C.; Saleh, S.; Unger, S.; van der Mey, D.; Mück, W. Clinical Pharmacokinetic and Pharmacodynamic Profile of Riociguat. *Clin. Pharmacokinet.* **2018**, *57*, 647–661.
- (33) Chen, Y.-J.; Ku, W.-C.; Feng, L.-T.; Tsai, M.-L.; Hsieh, C.-H.; Hsu, W.-H.; Liaw, W.-F.; Hung, C.-H.; Chen, Y.-J. Nitric Oxide Physiological Responses and Delivery Mechanisms Probed by Watersoluble Roussin's Red Ester and {Fe(NO)₂}¹⁰ DNIC. *J. Am. Chem. Soc.* 2008, *130*, 10929–10938.
- (34) Wu, S.-C.; Lu, C.-Y.; Chen, Y.-L.; Lo, F.-C.; Wang, T.-Y.; Chen, Y.-J.; Yuan, S.-S.; Liaw, W.-F.; Wang, Y.-M. Water-soluble Dinitrosyl Iron Complex (DNIC): a Nitric Oxide Vehicle Triggering Cancer Cell Death via Apoptosis. *Inorg. Chem.* **2016**, *55*, 9383–9392.
- (35) Huang, H.-W.; Lin, Y.-H.; Lin, M.-H.; Huang, Y.-R.; Chou, C.-H.; Hong, H.-C.; Wang, M.-R.; Tseng, Y.-T.; Liao, P.-C.; Chung, M.-C.; Ma, Y.-J.; Wu, S.-C.; Chuang, Y.-J.; Wang, H.-D.; Wang, Y.-M.; Huang, H.-D.; Lu, T.-T.; Liaw, W.-F. Extension of C. elegans Lifespan Using the NO-delivery Dinitrosyl Iron Complexes. *J. Biol. Inorg Chem.* 2018, 23, 775–784.
- (36) Adamyan, L. V.; Burgova, E. N.; Tkachev, N. A.; Mikoyan, V. D.; Stepanyan, A. A.; Sonova, M. M.; Galkin, A. V.; Vanin, A. F. Dinitrosyl Iron Complexes with Glutathione Largely Relieve Rats of Experimental Endometriosis. *Biophys. J.* **2013**, *58*, 222–227.
- (37) Burgova, E. N.; Tkachev, N. A.; Adamyan, L. V.; Mikoyan, V. D.; Paklina, O. V.; Stepanyan, A. A.; Vanin, A. F. Dinitrosyl Iron Complexes with Glutathione Suppress Experimental Endometriosis in Rats. *Eur. J. Pharmacol.* **2014**, *727*, 140–147.
- (38) Shamova, E. V.; Bichan, O. D.; Drozd, E. S.; Gorudko, I. V.; Chizhik, S. A.; Shumaev, K. B.; Cherenkevich, S. N.; Vanin, A. F. Regulation of the Functional and Mechanical Properties of Platelet and Red Blood Cells by Nitric Oxide Donors. *Biophys. J.* **2011**, *56*, 237–242.
- (39) Conrado, C. L.; Wecksler, S.; Egler, C.; Magde, D.; Ford, P. C. Synthesis and Photochemical Properties of a Novel Iron-sulfurnitrosyl Cluster Derivatized with the Pendant Chromophore Protoporphyrin IX. *Inorg. Chem.* **2004**, *43*, 5543–5549.
- (40) Fitzpatrick, J.; Kalyvas, H.; Filipovic, M. R.; Ivanović-Burmazović, I.; MacDonald, J. C.; Shearer, J.; Kim, E.; Kim, E. Transformation of a Mononitrosyl Iron Complex to a [2Fe-2S]

Cluster by a Cysteine Analogue. J. Am. Chem. Soc. 2014, 136, 7229–7232.

- (41) Tran, N. G.; Kalyvas, H.; Skodje, K. M.; Hayashi, T.; Moënne-Loccoz, P.; Callan, P. E.; Shearer, J.; Kirschenbaum, L. J.; Kim, E. Phenol Nitration Induced by a {Fe(NO)₂}¹⁰ Dinitrosyl Iron Complex. J. Am. Chem. Soc. **2011**, 133, 1184–1187.
- (42) Cesareo, E.; Parker, L. J.; Pedersen, J. Z.; Nuccetelli, M.; Mazzetti, A. P.; Pastore, A.; Federici, G.; Caccuri, A. M.; Ricci, G.; Adams, J. J.; Parker, M. W.; Bello, M. L. Nitrosylation of Human Glutathione Transferase P1-1 with Dinitrosyl Diglutathionyl Iron Complexin Vitroandin Vivo. *J. Biol. Chem.* **2005**, *280*, 42172–42180.
- (43) Pulukkody, R.; Chupik, R. B.; Montalvo, S. K.; Khan, S.; Bhuvanesh, N.; Lim, S.-M.; Darensbourg, M. Y. Toward Biocompatible Dinitrosyl Iron Complexes: Sugar-Appended Thiolates. *Chem. Commun.* **2017**, *53*, 1180–1183.
- (44) Elsabahy, M.; Samarajeewa, S.; Raymond, J. E.; Clark, C.; Wooley, K. L. Shell-crosslinked Knedel-like Nanoparticles Induce Lower Immunotoxicity than their Non-crosslinked Analogs. *J. Mater. Chem. B* **2013**, *1*, 5241.
- (45) Ignarro, L. J.; Fukuto, J. M.; Griscavage, J. M.; Rogers, N. E.; Byrns, R. E. Oxidation of nitric oxide in aqueous solution to nitrite but not nitrate: comparison with enzymatically formed nitric oxide from L-arginine. *Proc. Natl. Acad. Sci. U.S.A.* 1993, 90, 8103–8107.
- (46) Guven-Maiorov, E.; Acuner-Ozbabacan, S.; Keskin, O.; Gursoy, A.; Nussinov, R. Structural Pathways of Cytokines may Illuminate their Roles in Regulation of Cancer Development and Immunotherapy. *Cancers* **2014**, *6*, 663–683.
- (47) Elsabahy, M.; Li, A.; Zhang, F.; Sultan, D.; Liu, Y.; Wooley, K. L. Differential Immunotoxicities of Poly(ethylene glycol)- vs. Poly(carboxybetaine)-coated Nanoparticles. *J. Controlled Release* **2013**, 172, 641–652.
- (48) Elsabahy, M.; Shrestha, R.; Clark, C.; Taylor, S.; Leonard, J.; Wooley, K. L. Multifunctional Hierarchically Assembled Nanostructures as Complex Stage-wise Dual-delivery Systems for Coincidental yet Differential Trafficking of siRNA and Paclitaxel. *Nano Lett.* **2013**, 13, 2172–2181.
- (49) Elsabahy, M.; Wooley, K. L. Cytokines as Biomarkers of Nanoparticle Immunotoxicity. *Chem. Soc. Rev.* **2013**, 42, 5552–5576.
- (50) Elsabahy, M.; Zhang, S.; Zhang, F.; Deng, Z. J.; Lim, Y. H.; Wang, H.; Parsamian, P.; Hammond, P. T.; Wooley, K. L. Surface Charges and Shell Crosslinks Each Play Significant Roles in Mediating Degradation, Biofouling, Cytotoxicity and Immunotoxicity for Polyphosphoester-based Nanoparticles. *Sci. Rep.* **2013**, *3*, 3313.
- (S1) Stenken, J. A.; Poschenrieder, A. J. Bioanalytical Chemistry of Cytokines a Review. *Anal. Chim. Acta* **2015**, 853, 95–115.
- (52) Elsabahy, M.; Wooley, K. L. Data Mining as a Guide for the Construction of Cross-linked Nanoparticles with Low Immunotoxicity via Control of Polymer Chemistry and Supramolecular Assembly. *Acc. Chem. Res.* **2015**, *48*, 1620–1630.
- (53) Elsabahy, M.; Wooley, K. L. Reassessment of Nanomaterials Immunotoxicity. *Nano Today* **2018**, *20*, 10–12.
- (54) Elsabahy, M.; Wooley, K. L.; Hendricksen, A.; Oh, K. Multiplexing Techniques for Measurement of the Immunomodulatory Effects of Particulate Materials: Precautions when Testing Micro- and Nano-particles. *Methods* **2019**, *158*, 81–85.
- (55) He, W.; Frost, M. C. Direct Measurement of Actual Levels of Nitric Oxide (NO) in Cell Culture Conditions Using Soluble NO Donors. *Redox Biol.* **2016**, *9*, 1–14.